

Cite this: DOI:[10.56748/ejse.24439](https://doi.org/10.56748/ejse.24439)Received Date: 01 April 2023
Accepted Date: 08 February 2024

1443-9255

<https://ejsei.com/ejse>Copyright: © The Author(s).
Published by Electronic Journals
for Science and Engineering
International (EJSEI).This is an open access article
under the CC BY license.<https://creativecommons.org/licenses/by/4.0/>

Investigation on Residual Mechanical Properties of Galvanized Iron Cold-Formed Steel Sections Exposed to Elevated Temperatures

Varun Sam^a, N. Anand^{a*}, Garry Wegara K Marak^a, Garry Robson Lyngdoh^a, Johnson Alengaram^b, Diana Andrushia^c^a Department of Civil Engineering, Karunya university, Coimbatore, India^b Centre for Innovative Construction Technology (CICT), Department of Civil Engineering, Faculty of Engineering, University of Malaya, Kuala Lumpur, Malaysia^c Electronics and Communication Engineering, Karunya University, Coimbatore, India*Corresponding author: davids1612@gmail.com

Abstract

Cold-formed steel (CFS) sections are used to construct medium and low-rise structures designed to carry small-scale loads. CFS sections are manufactured without the application of heat. Therefore, it is crucial to comprehend the properties of CFS sections which are exposed to fire or elevated temperatures. To simulate the real-time fire exposure, an ISO Standard fire curve was used to heat the CFS sections. The objective of the study is to assess the residual mechanical strength of exposed sections after the elevated temperature test. The study aims to compile data for forecasting the degeneration of elements and to ascertain whether the structural components can be reused or replaced. The CFS sections were subjected to different temperatures, and after heating, two cooling methods were used to bring down to room temperature. The characteristics of the retrieved specimens, taken from exposed CFS sections were assessed using a tensile coupon test. The residual properties such as ultimate strength, yield strength, and elastic modulus were examined and reported. The influence of heating and cooling is more pronounced from the test results. A reduction in the yield and ultimate strength was noticed, and it was found to decrease as the heating intensity increases for air and water cooling respectively. In the case of yield and ultimate strength, the strength reduction is critical beyond 60 minutes. The elastic modulus was also found to be reducing with a similar trend. Based on the test results, reduction factors are proposed for ultimate strength, yield strength and elastic modulus. Reduction factors obtained for yield strength under 60 minutes of heating for air and water cooling is 0.575 and 0.557 respectively. In 120 minutes, the values are 0.400 and 0.329. Reduction factors obtained for ultimate strength under 60 minutes of heating for air and water cooling is 0.586 and 0.566 respectively. For 120 minutes, the values are 0.331 and 0.313.

Keywords

Cold-formed steel, Galvanized iron, Coupon test, Tensile strength, Mechanical properties

1. Introduction

Cold-form steel (CFS) is getting more popular day by day because of its high strength, availability, transportability, ease of construction, erection, ease of fabrication and lightweight. CFS sections are being used for various purposes, such as roofing, decking of floors, and basic elements of frames and panels. CFS sections are also called light gauge steel sections because of their lightweight. CFS sections are made from steel sheet rolls as shown in Fig. 1. It is bent into desired shapes and sizes without the application of heat.

The thickness of these sections varies between 1mm and 3mm. Coating sections with zinc or galvanizing may protect the section from corrosion and fire effects. The thickness of the coating depends on the environment and fire exposure. The usage of CFS sections increased in the last two decades for the construction of prefabricated framed buildings. Besides buildings, CFS is also used in the automotive and mechanical industries. CFS can be moulded to any desired shape and size. CFS elements can be joined together by any conventional method. The strength to weight ratio also is higher for CFS sections. It can be made of by stiffened or unstiffened, depending on the requirement. As well documented, the steel structures are vulnerable to fire. Therefore, it is crucial to study the behaviour of steel subjected to fire under different conditions. Depending on the magnitude, a fire can cause serious damage to life and properties. Such high fire magnitude is increasing at a steady state or transient condition in industrial structures like warehouses. Because of its thin nature, the CFS sections get more damage than hot rolled under fire. The use of cooling water is one of the most efficient ways to quench the fire, but it causes steel to reduce its stress capacity.

Research is underway to improve the load-bearing capacity of CFS sections under extreme fire conditions to ensure the fire safety of high-rise buildings and structures.

Galvanized Iron (GI) based cold form steel is getting popular in constructing warehouses, temporary hospitals and army bunkers because of its durability and ease of availability. In comparison to aluminum and

stainless steel, GI is cheaper and is available in various grades. The grade selection depends on the nature of the work and the strength requirements. Because of the added layer of zinc, the durability is high for GI-based CFS sections. It also protects the section from rust and corrosion (Karthick et al., 2020, Dewi et al., 2023). Since it does not need additional inspection, painting, or coating, it can be used immediately for field purposes. Maintenance is also very less for GI-based CFS sections. Without the galvanization iron, the steel can undergo oxidation, a chemical that deteriorates iron. The shiny appearance obtained by galvanizing can be used for aesthetic purposes in roofing.

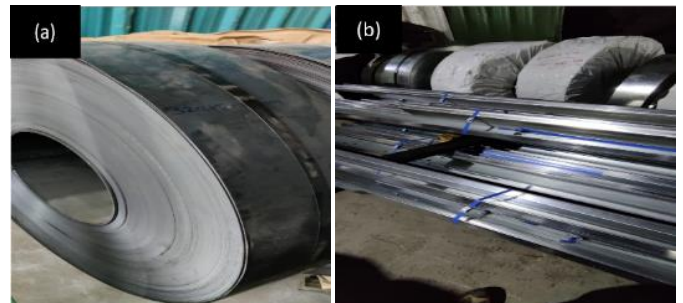


Fig. 1 (a) Coil of cold form steel (b) specimens made from sheets.

Researchers (Cheng et al., 2015, Gunalan et al., 2014, Kankanamge et al., 2011, Roy et al., 2021) have carried out extensive studies on the properties of CFS sections at high temperatures. They proposed strength reduction factors that were compared and correlated with values in fire codes. From the studies (Ren et al., 2020), samples that are cooled by water show better mechanical properties like Yield strength (YS), Ultimate strength (US), and Elastic modulus (EM) than the specimens which are cooled by air. It was concluded by researchers (Roy et al., 2019, Johnston et al., 2015) that the CFS sections are highly vulnerable under fire load.

Researchers (Cai & Young, 2014, Zheng et al., 2016, McCann et al., 2015) gave insights into properties like YS, US, and EM of CFS sections with

different shapes and sizes. Post-fire behaviour and residual mechanical properties of various types and grades of steel are studied by (Lu et al., 2016). The effect of different types of cooling and heating on various profiles and thickness of sections were investigated by many researchers (Zhang et al., 2020, Yan et al., 2021, Hanus et al., 2020, Yuan et al., 2016, H. T. Li et al., 2018).

Detailed studies have been conducted for coupon testing made with different materials under various testing conditions (Wang et al., 2015). Wang et al., 2010 analyzed various properties such as YS, US, and EM of low alloy steel, whereas (Azhari et al., 2015) studied the performance of steel tubes made of grade 1200. From past studies, the post-fire mechanical properties of high-strength steel were reduced. Post-fire behaviour of the high-strength steel section was investigated by (Pandey and Young., 2021). Mechanical response and creep strain of ultra-high strength grade steel subjected to different cooling conditions were studied by researchers (Azhari et al., 2015, Azhari et al., 2018). Post-fire behaviour of ultra-high strength steel was also studied by (Azhari et al., 2018). The strength reduction factors were determined for all these studies (Azhari et al., 2017b). Vandermaat et al., 2016 investigated laboratory-based coupon testing to examine stress corrosion cracking. The codes of practice CEN 2005 and BSI 1985 provide design guidelines for different properties of CFS sections subjected to high temperatures (CEN, 2005, BSI, 1985).

This paper investigates the mechanical properties of coupon specimens of unprotected CFS sections exposed to high temperatures, followed by the ISO 834 standard fire curve (ISO 834-1, 1999). The specimens were then made to cool by using air or water. After cooling the specimens, they were observed for any physical changes. The failures and their pattern were noted to assess the damage obtained during the fire exposure. A detailed analysis has been made to evaluate the YS, US, EM, stress-strain behaviour, and ductility of CFS exposed sections.

Researchers have done past studies on steel sections heated to different temperatures and tested them to check their strength properties (G. Q. Li et al., 2017, Mushahary et al., 2021). Fig. 2 shows nominal YS obtained from a different steel grade based on past research works. Researchers (Hanus et al., 2020, Kesawan & Mahendran, 2018, Singh & Singh., 2019) found out YS of various grades of steel under different loading conditions. Almost all the grades have YS above 350 (Yan et al., 2021, W. Wang et al., 2015). It is the observation that research on GI-based CFS sections is very limited, so it is vital to understand more about the fire resistance capacity of GI steel sections.

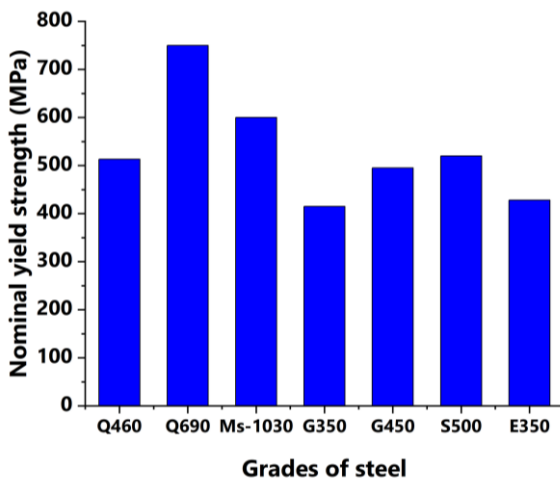


Fig. 2 Nominal yield strength obtained for different grades of steel sections.

Understanding the effect of fire exposure on CFS sections will be helpful for a design application in the CFS-based structural elements. The influence of temperature exposure highly affects sections' physical and mechanical performance. Due to this, significant reductions can be observed in the elastic modulus and yield strength of sections. However, the extent of damage and its effect on material strength for CFS sections

Table 1 Section properties

Section dimensions (mm)	Weight (kg/m)	Area (cm ²)	Thickness (mm)	Moment of inertia in X direction I_{xx} (cm ⁴)	Moment of inertia in Y direction I_{yy} (cm ⁴)	Radius of gyration about X-axis (cm)	Radius of gyration about Y-axis (cm)
200x60x20	5.42	6.80	2	403.96	29.65	7.71	2.09

under higher temperatures is rarely reported. Industrial purlins are primarily made up of CFS elements with various profiles. The influence of cooling effect on strength properties of CFS sections are to be investigated. Under extreme fire events, the CFS elements may undergo failure before reaching their limit state. Considering this information from past studies, the proposed investigation aims to analyze the mechanical performance of CFS sections after exposure to elevated temperature.

2. Experimental Investigation

2.1 Properties of the test specimen

Numerous types of CFS sections like mild steel, stainless steel, aluminium are used for construction purposes. GI-based CFS sections of grade 350 were utilized in the experiments to evaluate its performance under fire exposure. The coupon specimens were taken from the CFS beam of back-to-back C-sections with dimensions of 200 x 60 x 60 x 20mm and a length of 1.5m. Table 1 shows the section properties of the material that was utilized for conducting the investigation. Fig. 3 shows the GI-based CFS C section used to extract coupon specimens.



Fig. 3 GI-based cold form steel beam sections

2.2 Heating and cooling procedure of CFS specimen

The furnace used for heating the CFS specimen is an electrically operated, computer-based temperature-controlled type. Heating coils are embedded on the sides of the furnace. The furnace has dimensions of 700 x 400 x 400 mm. According to ISO 834 fire curve (ISO 834-1, 1999) which is shown in Fig. 9, all specimens were allowed to heat up to desired temperatures. Specimens were placed in the furnace to provide even temperature distribution across the specimen. The maximum operating temperature is 1300°C. A computerized control panel is used to regulate the rate of heating. The CFS beam sections were heated at 690°C, 821°C, 882°C, 925°C, 986°C and 1029°C, respectively, under transient state conditions for various periods such as 15, 30, 45, 60, 90, and 120 minutes. For instance, 15AC represents the specimens heated up to 15minutes and cooled with air cooling (AC). Similarly, 15WC represents the specimens heated up to 15minutes and cooled with water cooling (WC). Fig. 4 shows the furnace which was used for the elevated temperature test. After heating, the specimens were taken from the furnace and left for cooling at room temperature or by water before testing. The thermocouples connected to the main control unit were used to monitor the temperature readings periodically throughout the heating process. Fig. 5 shows the cooling of the specimen using water and the C section kept inside the furnace for cooling under natural air.



Fig. 4 (a) Heating coils inside furnace (b) Furnace used for heating specimens.

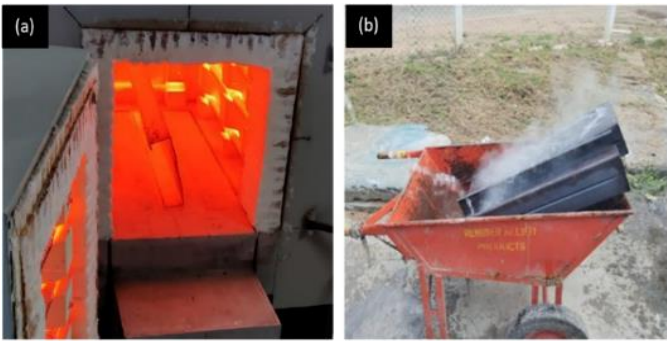


Fig. 5 (a) Specimen exposed to elevated temperature using furnace (b) Specimen cooled by water cooling.

2.3 Preparation of specimens used for coupon test

The CFS C sections were utilized to extract the tensile test coupon specimens to assess their properties. After the steel beam specimens are heated and cooled, coupon specimens are extracted from the beam along the longitudinal direction at the middle and side parts of the web. A wire EDM machine is used to extract specimens which are shown in Fig. 7. The extracted dimensions were based on specifications mentioned in ASTM E8 standards (ASTM, 2021). Fig. 6 shows extracted specimen as well as its dimensions.

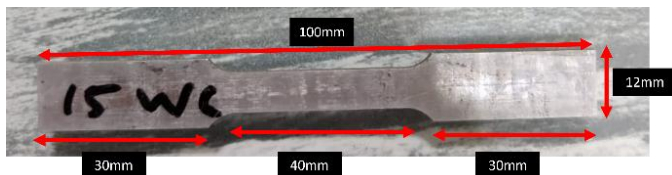


Fig. 6 Schematic view of coupon specimen, sample coupon specimen.

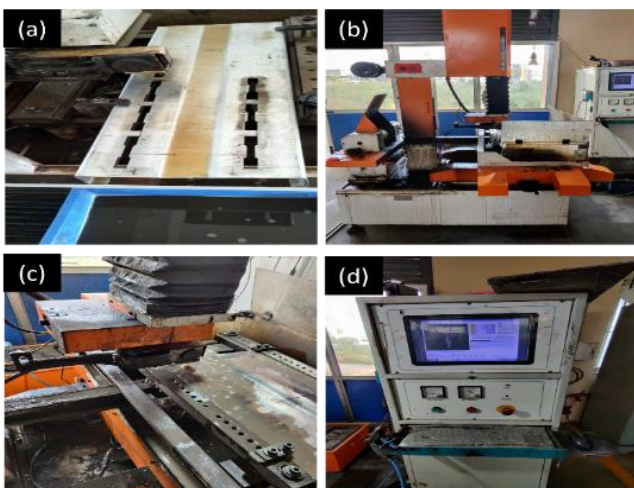


Fig. 7 (a) Specimen being extracted from EDM, (b) Wire EDM machine, (c) Cutting process, (d) Input for Wire EDM machine.

2.4 Tensile coupon test

After the specimens are heated, they are cooled either using natural air or water. After cooling down, the specimens were used for tensile coupon test with a computerized universal testing machine with a capacity of 1000 kN to find properties of GI steel as shown in Fig. 8. The rate of load, which is constantly applied till the failure of the specimen, is 0.5mm/minute in a load control manner. Strain values are monitored using a strain gauge (HBM: test and measurement) connected to the specimens' center part. The strain gauge of 50mm length and 120Ω resistance is used. It was connected to the neck area of the specimen. The strain dataset is indicated by the method of quarter-bridge circuit connection. The values were taken and observed in a digital strain data logger till the failure of the specimen. A computerized data acquisition system monitors load and displacement values at certain intervals. By using a recorded data set, the graphs were plotted. The values of strain are monitored till 2% of proof stress. After the failure of the test specimen, the elongation of steel is measured using a micrometer. YS, US, strain at fracture, and EM values were calculated from the test data.

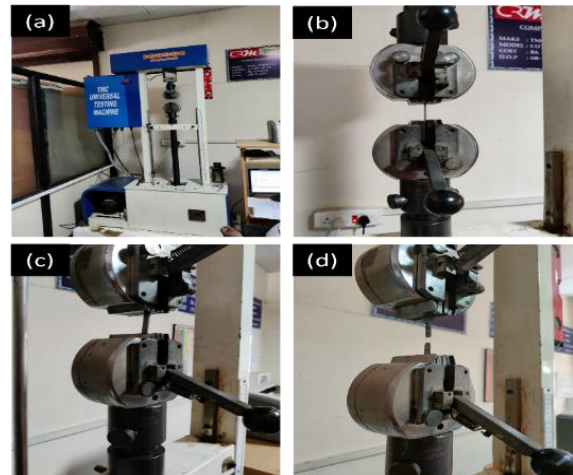


Fig. 8 (a) UTM machine used for tensile testing (b) (c) Placement of specimen in UTM machine (d) Failure of the specimen.

3. Results and Discussion

3.1 Time and temperature measurements

Time and temperature values were recorded, and values of temperature were observed at two different locations; one is on the coil of the furnace, which can be termed as CFST1. Another is on the surface of the beam specimen, namely CFST2. The values of temperature on the specimen as well as on the coil were recorded using K-type thermocouples attached to a microprocessor control unit shown in Fig. 10. The furnace gets automatically off after the desired temperature is attained, and the time-temperature values are measured in a microprocessor-controlled data acquisition device.

ISO fire curve is used for heating the specimens, the set target temperatures are based on the readings given in ISO 834 guidelines. The temperature value changes based on duration of heating. The applied temperature and the coil temperature are similar, and it is recorded by control panel. From the readings shown on microprocessor, it can be confirmed that the temperature applied on the coil is same as per the values given in standard fire curve. The temperature measured on the specimen is like that of the coil, with a marginal difference. During the first 10 minutes, a minute difference in temperature of about 3.25-5.7% is noted. The temperature, which is measured for all specimens at the CFST1 location and CFST2 location, was recorded with minute change.

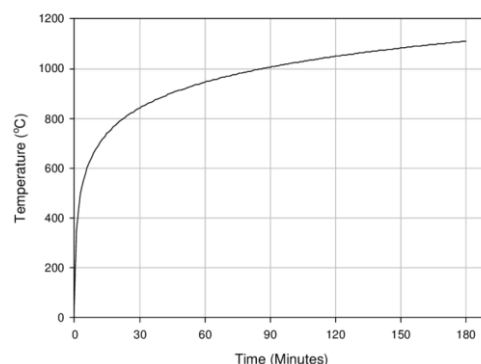


Fig. 9 ISO 834 Standard Fire Curve.



Fig. 10 Position of Thermocouple.

3.2 Failure pattern of coupon specimens

To understand the intensity of damage due to fire exposure, it is vital to study changes in the physical aspects of failed specimens. The texture on the surface of the specimens, level of damage on the specimens, and changes in colour with gradient are observed. It can be concluded that the damage to the texture of the surface and changes in colour are directly proportional to the period of heating. After heating the coupon specimen, colour changes were seen in specimens heated at high periods. The colour changed to dark grey for high durations of heating. Flaking also was seen in such specimens. For lower durations, there was no notable change in colour.

Fig. 11 shows the failure pattern of specimens subjected to tensile load test; failure was observed within the gauge length for all the specimens. Necking was seen for all the specimens before failing. The observed tensile fracture is smooth during the first 30 minutes (821°C) of heat application. After this point, i.e., at 45 (882°C), 60 (925°C), 90 (986°C) and 120 minutes (1029°C), the surface became rough, and a pattern of failure was visible at the fracture of the specimen. This could be due to the gain in the larger duration of heating of specimen. This effect was observed with a brittle mode of failure. The tempering effect of steel occurs above 30 minutes and ferrites are formed (Yan et al., 2021). For specimens heated to 120 minutes, the noted failure mode was brittle with random necking for both the cooling conditions. Similar observations are reported elsewhere (Lu et al., 2016).



Fig. 11 Failure pattern of the coupon specimens tested.

3.3 Stress-strain behaviour

The stress-strain behaviour of CFS steel specimens was obtained from the coupon test. The stress-strain curves obtained for the specimens of water and air-cooled are shown in Fig. 12. The graph shows that the reference specimen shows a particular linear elastic region which leads to an incremental yielding (Chen et al., 2007, Ranawaka & Mahendran, 2009). The effect of temperature significantly influences stress-strain behaviour, yield, and ultimate strength. The decline in mechanical stress response and strain increase was observed while the heating time increased.

The YS of steel is inversely proportional to the increased duration of heating. The strain values are more for high durations of heating and less for lower durations. A higher strain hardening range was observed during the decline in stress capacity under prolonged exposure. An increase in the strain of about 1.35 times was noted for 60-minute air-cooled sections concerning the reference section. For 120 minutes, the recorded increase was 1.53 times more than the reference section. The effect of the cooling process is more pronounced in the reduction in stress capacity and strain increment. In the water-cooling process, the increments in strain value are almost like specimens cooled using air. The changes in yield and the ultimate and elastic modulus of CFS are explained in the following sections.

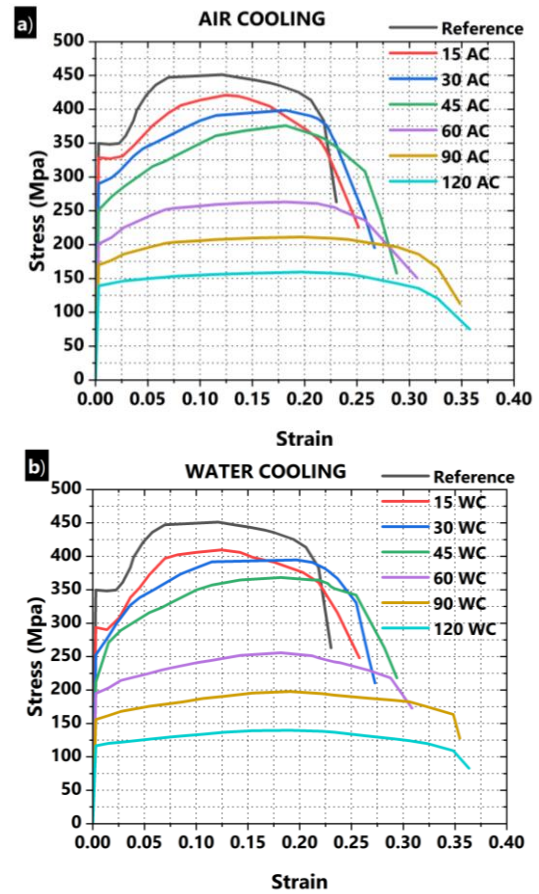


Fig. 12 Stress-strain response of CFS sections a) Air-cooled CFS b) Water-cooled CFS.

3.4 Yield strength

Yield strength (YS) has a major effect in deciding the strength of steel structures. Therefore, YS is vital in designing and modelling the sections. Steel sections possess higher ductility due to their yielding capacity under tensile stresses than other materials used for construction. The YS of steel specimens exposed to temperature is shown in Fig. 13. The results from the tests are noted down based on the duration of heating and cooling. The reduction in yield strength is dependent on rate of heating and process of cooling. Beyond 30 minutes of heating, strength loss is critical, because the material strength is significantly reduced. This reduction in strength affects the material safety factor to be considered for the design. Reduction factor is the ratio between strength of heated specimen to unheated specimen. For all the strength values of different heating conditions the reference values in considered as a benchmark for comparison of performance. This reduction factor is calculated for yield strength, ultimate strength, and elastic modulus in the presented paper. Reduction factor values for YS for each specimen are shown in Fig. 13.

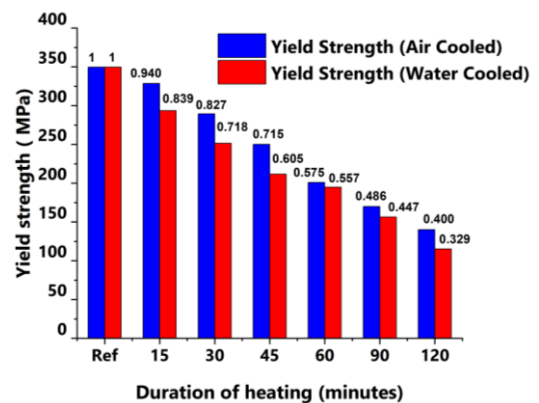


Fig. 13 Yield strength and its reduction factor of CFS sections which are air and water-cooled.

The experimental results reveal that specimens cooled by water had a higher strength loss than those cooled by air. From the graph, it is evident that YS decreases with the increase in temperature. Up to 15 minutes, the loss is marginal, but above 15 minutes, the loss is significant for both cases of cooling.

The obtained strength reduction is more for specimens cooled by water. The results are comparable with the reports of (Lu et al., 2016). Specimens cooled using water had higher strength loss because of its sudden thermal shock and steep temperature gradient compared to air cooling (Sabu Sam et al., 2023). Differences in cooling methods can significantly affect the material properties and behaviour of the specimens. Rapid cooling creates non-uniform temperature gradients within the material. This non-uniform cooling leads to non-uniform contraction and the development of residual stresses within the material. While air cooling may still induce some residual stresses and microstructural changes, the effects are generally less severe than with using water.

3.5 Ultimate strength

Fig. 14 shows the US values in various stages of heating and cooling. The reduction rate in the US is directly proportional to the duration of heating. An increase in magnitude and duration of heating had a great impact on US of specimens. Prolonged duration and water-cooling process affects the ultimate strength of the material. Due to the degradation of US, the failure pattern of structural elements may change and thus lead to premature collapse under loading. For a long duration of heating, the specimens exposed for 120 minutes show a larger strength loss which is because of the steep temperature gradient (Ren et al., 2020, Chen et al., 2007). The pattern of strength reduction follows here, too, which shows that specimens cooled using water have higher strength loss. Reduction factors for each specimen are displayed in Fig. 14.

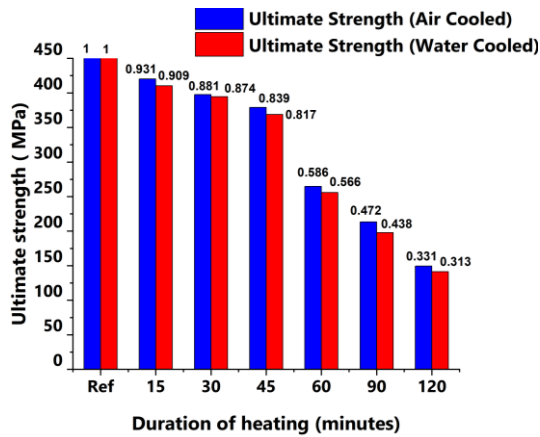


Fig. 14 Ultimate strength and its reduction factor of CFS sections

3.6 Elastic modulus

Fig. 15 shows the EM values of specimens which are heated and cooled under using air and water. The EM was obtained from the initial slope of the stress-strain graph. The elastic and plastic regions are seen for both the unheated as well as heated specimens. During the initial phase of heating at 15 and 30 minutes, there was a reduction in strength for all the specimens. During the 60 minutes of heating, the specimens showed greater strength loss for all types of specimens. The reduction rate of EM is directly proportional to YS loss (Kumar et al., 2022). The reduction in stress capacity and increase in strain under the exposure affects the elastic modulus of the specimens. The influence of temperature and its effect on EM, can reduce the bending capacity of elements under transverse loading. Also, the members may fail due to larger deflection profile under higher duration of heating. EM of CFS specimens cooled using water is lower than the values of specimens cooled using air. Reduction factors for each specimen are displayed in Fig. 15.

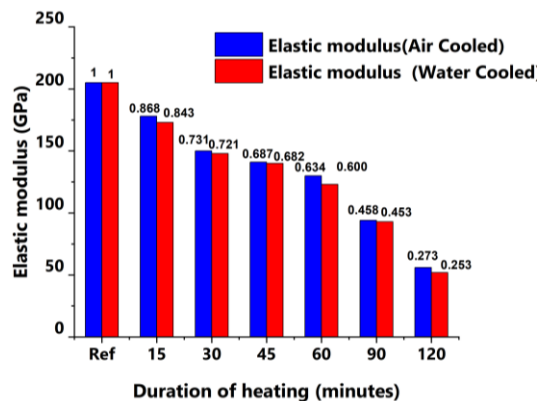


Fig. 15 Elastic modulus and its reduction factor of CFS sections

4. Reduction factor (RF)

4.1 RF of GI-based CFS section.

The strength of heated specimens divided by the strength of reference specimens can be termed as the reduction factor. From the test conducted, reduction factors for YS, US and EM are obtained. Many researchers (Ren et al., 2020, Yu et al., 2019, Kesawan et al., 2018, G. Q. Li et al., 2017, H. T. Li et al., 2018, W. Wang et al., 2015, Hanus et al., 2020, Mushahary et al., 2021) studied the behaviour of coupons of various grades of steel.

From reviewing past works, it's clear that there is a hike in strength for temperatures between 200 and 5000 C. For temperatures 900oC and above, there was a strength loss due to high temperature, as seen in Figs 13, 14 and 15 (Singh et al., 2019, Yuan et al., 2016).

From the data obtained, the reduction factor goes down with the increase in the period of heating. The reduction factor of specimens cooled under air was slightly higher than those cooled with water. Similar patterns were seen in the reduction factors of YS, US and EM. The reduction factor of YS starts from 0.94 for 15 minutes and is further reduced to 0.400 for 120 minutes in air-cooled specimens. For water-cooled specimens' the reduction factor starts from 0.839 for 15 minutes and is reduced to 0.329 for 120 minutes.

Similarly, for US, the highest reduction factor of 0.931 was obtained for 15 minutes and reduced to 0.331 for 120 minutes in air-cooled specimens. For the water-cooled case, it is between 0.909 and 0.313. In the case of EM, the air-cooling case values were between 0.868 and 0.273. For water cooling, it was between 0.843 and 0.253. The reduction factor values of strength parameters (for different heating-cooling cases) may be helpful for design applications. This gives an idea about the factor of safety one should consider during the design of members under extreme fire conditions.

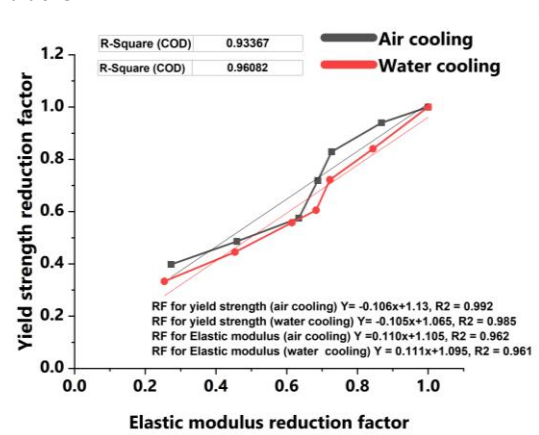


Fig. 16 Relationship with reduction factor of Yield strength with Elastic modulus in air- and water-cooled specimens

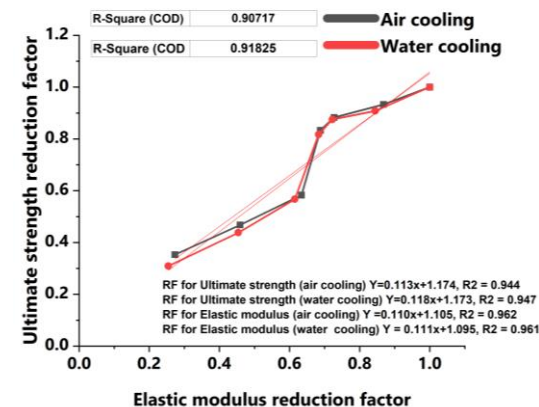


Fig. 17 Relationship with reduction factor of Elastic modulus with ultimate strength in air- and water-cooled specimens

In Figs 16 and 17, there was a correlation between the reduction factor of EM with the reduction factor of YS and US of specimens cooled by air and water. In the graphs, a linear relationship is obtained between the reduction factor of EM with the reduction factor of US and YS. In the relationship between the reduction factor of EM and YS, a sudden drop was observed after 30 minutes of heating. In the case of US, the sudden reduction starts from 45 minutes to 120 minutes. A positive linear correlation has been obtained between these strength parameters and displayed in the graphs, and the R2 values are nearly equal to 1.

In these Figs, empirical equations are displayed which can be used for determining the reduction factor of mechanical properties such as YS, EM, and US. The proposed relation can be used for structural design application, in the case of evaluating residual mechanical properties.

5. Conclusions

A detailed study has been made on the properties of CFS galvanized iron specimens subjected to standard heat exposure. The specimens were heated for various time periods 15, 30, 45, 60, 90 and 120 minutes. After heating, the specimens were made to cool using air or water.

From the study, physical properties, failure pattern, stress-strain behaviour, YS, US, EM, and RF were obtained. The conclusions which are obtained from this study are as follows.

The specimens exhibited colour changes as the time for exposure temperature increased. The specimens turned to dark grey colour as the duration of heating was increased. For smaller durations, there were no significant colour changes observed.

The mechanical properties are affected by the duration of heating and the way of cooling. There was a change in almost all the properties of the CFS section. Flaking was seen on the surface of some of the specimens as the duration of heating increased.

It is noted that yield strength was reduced as the applied temperature becomes higher. A similar trend has been observed for ultimate strength and elastic modulus also. However, the reduction in strength depends on rate of heating, duration, and process of cooling.

It is noted that among all the properties investigated, air-cooled specimens showed better results than the water-cooled specimens.

The reduction factors are proposed for ultimate strength, yield strength, and elastic modulus. A statistical relationship is also proposed between reduction factors of yield strength and ultimate strength with the reduction factor of elastic modulus.

The reduction factor obtained for ultimate strength under 60 minutes of heating for air and water cooling is 0.586 and 0.566 respectively. For 120 minutes, the values are 0.331 and 0.313. The reduction factor obtained for yield strength under 60 minutes of heating for air and water cooling is 0.575 and 0.557 respectively. In 120 minutes, the values are 0.400 and 0.329.

Further, experiments can be done for stainless steel sections exposed to an elevated temperature to determine the residual mechanical properties.

6. Reference

ASTM. (2021). ASTM E8/E8M standard test methods for tension testing of metallic materials. Annual Book of ASTM Standards, C.

Azhari, F., Heidarpour, A., Zhao, X. L., & Hutchinson, C. R. (2015). Mechanical properties of ultra-high strength (Grade 1200) steel tubes under cooling phase of a fire: An experimental investigation. *Construction and Building Materials*, 93. <https://doi.org/10.1016/j.conbuildmat.2015.05.082>

Azhari, F., Heidarpour, A., Zhao, X. L., & Hutchinson, C. R. (2017a). Effect of creep strain on mechanical behaviour of ultra-high strength (Grade 1200) steel subject to cooling phase of a fire. *Construction and Building Materials*, 136. <https://doi.org/10.1016/j.conbuildmat.2017.01.025>

Azhari, F., Heidarpour, A., Zhao, X. L., & Hutchinson, C. R. (2017b). Post-fire mechanical response of ultra-high strength (Grade 1200) steel under high temperatures: Linking thermal stability and microstructure. *Thin-Walled Structures*, 119. <https://doi.org/10.1016/j.tws.2017.05.030>

Azhari, F., Hossain Apon, A. A., Heidarpour, A., Zhao, X. L., & Hutchinson, C. R. (2018). Mechanical response of ultra-high strength (Grade 1200) steel under extreme cooling conditions. *Construction and Building Materials*, 175. <https://doi.org/10.1016/j.conbuildmat.2018.04.191>

BSI. (1985). BS5950-8:2003: Structural Use of steelwork in building: Part 8: Code of practice for fire resistant design. Part, 3(1).

Cai, Y., & Young, B. (2014). Behavior of cold-formed stainless steel single shear bolted connections at elevated temperatures. *Thin-Walled Structures*. <https://doi.org/10.1016/j.tws.2013.10.010>

CEN. (2005). Eurocode 3: Design of steel structures - Part 1-2: General rules - Structural fire design. *Journal of Constructional Steel Research*, 54(2).

Chen, J., & Young, B. (2007). Experimental investigation of cold-formed steel material at elevated temperatures. *Thin-Walled Structures*, 45(1), 96–110. <https://doi.org/10.1016/j.tws.2006.11.003>

Cheng, S., Li, L. Y., & Kim, B. (2015). Buckling analysis of cold-formed steel channel-section beams at elevated temperatures. *Journal of Constructional Steel Research*, 104, 74–80. <https://doi.org/10.1016/j.jcsr.2014.10.004>

Dewi, M. S., Sancharoen, P., Klomjit, P., & Tangtermsirikul, S. (2023). Effects of Zinc alloy layer on corrosion and service life of galvanized

reinforcing steels in chloride-contaminated concrete. *Journal of Building Engineering*, 68, 106153. <https://doi.org/10.1016/j.jobe.2023.106153>

Gunalan, S., & Mahendran, M. (2014). Experimental and numerical studies of fire exposed lipped channel columns subject to distortional buckling. *Fire Safety Journal*, 70, 34–45. <https://doi.org/10.1016/j.firesaf.2014.08.018>

Hanus, F., Caillet, N., Gaillard, S., & Vassart, O. (2020). Strength reduction factors for S355 to S500 steel grades under steady-state and transient-state heating. *Journal of Structural Fire Engineering*. <https://doi.org/10.1108/JSFE-01-2019-0001>

ISO 834-1. (1999). Fire-resistance tests - Elements of building construction - Part 1: General requirements. ISO Standard, STD-615580.

Johnston, R. P. D., Sonebi, M., Lim, J. B. P., Armstrong, C. G., Wrzesien, A. M., Abdelal, G., & Hu, Y. (2015). The collapse behaviour of cold-formed steel portal frames at elevated temperatures. *Journal of Structural Fire Engineering*. <https://doi.org/10.1260/2040-2317.6.2.77>

Kankanamge, N. D., & Mahendran, M. (2011). Mechanical properties of cold-formed steels at elevated temperatures. *Thin-Walled Structures*, 49(1), 26–44. <https://doi.org/10.1016/j.tws.2010.08.004>

Karthick, S., Muralidharan, S., & Saraswathy, V. (2020). Corrosion performance of mild steel and galvanized iron in clay soil environment. *Arabian Journal of Chemistry*, 13(1), 3301–3318. <https://doi.org/10.1016/j.arabjch.2018.11.005>

Kesawan, S., & Mahendran, M. (2018). Post-fire mechanical properties of cold-formed steel hollow sections. *Construction and Building Materials*. <https://doi.org/10.1016/j.conbuildmat.2017.11.077>

Kumar, G. J., Kiran, T., & Anand, N. (2022). Influence of fire-resistant coating on the physical characteristics and residual mechanical properties of E350 steel section exposed to elevated temperature. <https://doi.org/10.1108/JSFE-02-2022-0008>

Li, G. Q., Lyu, H., & Zhang, C. (2017). Post-fire mechanical properties of high strength Q690 structural steel. *Journal of Constructional Steel Research*. <https://doi.org/10.1016/j.jcsr.2016.12.027>

Li, H. T., & Young, B. (2018). Residual mechanical properties of high strength steels after exposure to fire. *Journal of Constructional Steel Research*. <https://doi.org/10.1016/j.jcsr.2018.05.028>

Lu, J., Liu, H., Chen, Z., & Liao, X. (2016). Experimental investigation into the post-fire mechanical properties of hot-rolled and cold-formed steels. *Journal of Constructional Steel Research*. <https://doi.org/10.1016/j.jcsr.2016.03.005>

McCann, F., Gardner, L., & Kirk, S. (2015). Elevated temperature material properties of cold-formed steel hollow sections. *Thin-Walled Structures*. <https://doi.org/10.1016/j.tws.2015.01.007>

Mushahary, S. K., Singh, K. D., & Jayachandran, S. A. (2021). Mechanical properties of E350 steel during heating and cooling. *Thin-Walled Structures*. <https://doi.org/10.1016/j.tws.2020.107351>

Pandey, M., & Young, B. (2021). Post-fire mechanical response of high strength steels. *Thin-Walled Structures*, 164. <https://doi.org/10.1016/j.tws.2021.107606>

Ranawaka, T., & Mahendran, M. (2009). Experimental study of the mechanical properties of light gauge cold-formed steels at elevated temperatures. *Fire Safety Journal*. <https://doi.org/10.1016/j.firesaf.2008.06.006>

Ren, C., Dai, L., Huang, Y., & He, W. (2020). Experimental investigation of post-fire mechanical properties of Q235 cold-formed steel. *Thin-Walled Structures*. <https://doi.org/10.1016/j.tws.2020.106651>

Roy, K., Ho Lau, H., Ting, T. C. H., Chen, B., & Lim, J. B. P. (2021). Flexural behaviour of back-to-back built-up cold-formed steel channel beams: Experiments and finite element modelling. *Structures*. <https://doi.org/10.1016/j.istruc.2020.10.052>

Roy, K., Lim, J. B. P., Lau, H. H., Yong, P. M., Clifton, G. C., Wrzesien, A., & Mei, C. C. (2019). Collapse behaviour of a fire engineering designed single-storey cold-formed steel building in severe fires. *Thin-Walled Structures*, 142, 340–357. <https://doi.org/10.1016/j.tws.2019.04.046>

Sabu Sam, V., Adarsh, M. S., Lyngdoh, G. R., Marak, G. W. K., Anand, N., Al-Jabri, K., & Andrushia, D. (2023). Influence of elevated temperature on buckling capacity of mild steel-based cold-formed steel column sections—experimental investigation and finite element modelling. *Journal of Structural Fire Engineering*, ahead-of-print(ahead-of-print). <https://doi.org/10.1108/JSFE-08-2023-0033>

Singh, T. G., & Singh, K. D. (2019). Mechanical properties of YSt-310 cold-formed steel hollow sections at elevated temperatures. *Journal of Constructional Steel Research*. <https://doi.org/10.1016/j.jcsr.2019.03.004>

Vandermaat, D., Saydam, S., Hagan, P. C., & Crosky, A. (2016). Laboratory-based coupon testing for the understanding of SCC in rockbolts. *Transactions of the Institutions of Mining and Metallurgy, Section A: Mining Technology*, 125(3), 174–183. <https://doi.org/10.1080/14749009.2015.1122296>

Wang, L., Cai, Q., Yu, W., Wu, H., & Lei, A. (2010). Microstructure and mechanical properties of 1500 MPa grade ultra-high strength low alloy steel. *Jinshu Xuebao/Acta Metallurgica Sinica*, 46(6). <https://doi.org/10.3724/SP.J.1037.2010.00687>

Wang, W., Liu, T., & Liu, J. (2015). Experimental study on post-fire mechanical properties of high strength Q460 steel. *Journal of Constructional Steel Research*. <https://doi:10.1016/j.jcsr.2015.07.019>

Yan, X., Xia, Y., Blum, H. B., & Gernay, T. (2021). Post-fire mechanical properties of advanced high-strength cold-formed steel alloys. *Thin-Walled Structures*. <https://doi:10.1016/j.tws.2020.107293>

Yu, Y., Lan, L., Ding, F., & Wang, L. (2019). Mechanical properties of hot-rolled and cold-formed steels after exposure to elevated temperature: A review. In *Construction and Building Materials*. <https://doi:10.1016/j.conbuildmat.2019.04.062>

Yuan, G., Shu, Q., Huang, Z., & Li, Q. (2016). An experimental investigation of properties of Q345 steel pipe at elevated temperatures. *Journal of Constructional Steel Research*. <https://doi:10.1016/j.jcsr.2015.10.022>

Zhang, C., Wang, R., & Song, G. (2020). Post-fire mechanical properties of Q460 and Q690 high strength steels after fire-fighting foam cooling. *Thin-Walled Structures*. <https://doi:10.1016/j.tws.2020.106983>

Zheng, B., Shu, G., Xin, L., Yang, R., & Jiang, Q. (2016). Study on the Bending Capacity of Cold-formed Stainless Steel Hollow Sections. *Structures*. <https://doi:10.1016/j.istruc.2016.08.007>